Inorg. Chem. **2008**, *47*, 9561−9568

Spacer-Directed Coordination Polymers-of-Oligomers (POLO) of Silver

Peili Teo, L. L. Koh, and T. S. Andy Hor*

Department of Chemistry, National University of Singapore, 3 Science Drive 3, Singapore 117543

Received July 14, 2008

A novel series of Ag(I) polymers-of-oligomers with pyridylcarboxylate spacers supported by a diphosphine [1,1′-bis(diphenylphosphino)methane (dppm) or 1,1′-bis(diphenylphosphino)ferrocene (dppf)] has been constructed and crystallographically established. The repeating oligomeric Ag_5 block is invariably made up of five Ag(I) centers comprising Ag_2 and Ag units with different metal geometries. Other related Ag_5 and Ag_4 assemblies have also been isolated. The preparation of the $[Ag_2(isonic)(dppm)_2]_n^{n+}$ polymer (isonic = 4-pyridyl formate, $NC_5H_4CO_2^-$) using a ligand transfer pathway from $NiCl_2(dppm)$ to AgOTf (OTf = $CF_3SO_3^-$) has been identified. The structural outcomes suggested that pyridylcarboxylates of different stereogeometrical and conformational properties can stabilize different oligomeric and topological forms through adaptation to the contrasting demands of the diphosphine and metal.

Introduction

Self-assemblies of Ag(I) polymers are of topical interest because of their structural,[1] electronic,[2] and photophysical[3] properties as well as their wide-ranging nano applications.[4] Further development of these complexes as advanced materials will hinge on the ability to design and synthesize structurally defined systems that inherit specific network-dependent material properties. Our ongoing interest in the coordination chemistry of coinage metals, especially Ag(I),[5] has recently led to the development of hybrid and bifunctional ligands such as pyridyl carboxylates[6] as spacers to control the directionality of nuclearity growth. This is a formidable challenge in Ag(I) assembly because, unlike the likes of d^6 or d^8 metals, it has a dynamic range of coordinative variations such as linear, trigonal-planar, T-shaped, tetrahedral, mono- and polymeric formation, di- versus oligomerization, with or without argentophilic interactions, intra- and intermolecular coordination, and so forth. These give rise to a myriad of unpredictable, uncontrollable, and at times uncharacterizable assemblies. We shall highlight in this paper how a combinative use of the donor and spatial features of pyridylcarboxylates and diphosphine could cooperatively direct to specific oligomeric assemblies and their polymeric forms.

Results and Discussion

Attempts to prepare $[Ni(isonic)(dppm)]^+$ (dppm = 1,1′-bis(diphenylphosphino)methane) from a metathesis reaction of $NiCl_2(dppm)$/AgOTf with 4-pyridyl formic acid (isonicH) resulted in a coordination polymer $[Ag_2(isonic)(dppm)_2]_n(OTf)_n$, **1** (isonic = 4-pyridyl formate, $NC_5H_4CO_2^-$, and OTf = $CF_3SO_3^-$; Figure 1, Table 1). A similar reaction using $NiX_2(dppe)$ gives rise to phosphine migration to Ag(I)[5c] but

* Authors to whom correspondence should be addressed. Tel: 65 65162679. Fax: 65 65162663. E-mail: andyhor@nus.edu.sg.

(1) (a) Kuang, S.-M.; Zhang, Z.-Z.; Wang, Q.-G.; Mak, T. C. W. *Chem. Comm.* **1998**, 581. (b) Zhao, X.-L.; Mak, T. C. W. *Organometallics* **2005**, *24* (19), 4497. (c) Argent, S. P.; Adams, H.; Johannessen, T. R.; Jefferey, J. C.; Harding, L. P.; Harrington, R. W.; Ward, M. D. *Dalton Trans.* **2006**, 4996. (d) Yue, N. L. S.; Jennings, M. C.; Puddephatt, R. J. *Inorg. Chem.* **2005**, *44*, 1125.

(2) Liu, S. Q.; Sowa, T. K.; Konaka, H. Y.; Suenaga, H.; Maekawa, M.; Mizutani, T.; Ning, G. L.; Munakata, M. *Inorg. Chem.* **2005**, *44*, 1031.

(3) (a) Liu, Z.; Liu, P.; Chen, Y.; Wang, J.; Huang, M. *New J. Chem.* **2005**, *29*, 474. (b) Sun, D.; Cao, R.; Weng, J.; Hong, M.; Liang, Y. *Dalton Trans.* **2002**, 291. (c) Fortin, D.; Drouin, M.; Turcotte, M.; Harvey, P. D. *J. Am. Chem. Soc.* **1997**, *119*, 531. (d) Lin, R.; Yip, J. H. K. *Inorg. Chem.* **2006**, *45*, 4423. (e) Yam, V. W.; Fung, W. K.; Cheung, K. *Chem. Comm.* **1997**, 963.

(4) (a) Zhang, J.-P.; Kitagawa, S. *J. Am. Chem. Soc.* **2008**, *130*, 907. (b) Fan, J.; Wang, Y.; Blake, A. J.; Wilson, C.; Davies, E. S.; Khlobystov, A. N.; Schroder, M. *Angew. Chem., Int. Ed.* **2007**, *46*, 8013. (c) Zhang, J.-P.; Horike, S.; Kitagawa, S. *Angew. Chem., Int. Ed.* **2007**, *46*, 889.

(5) (a) Lu, X. L.; Leong, W. K.; Hor, T. S. A.; Goh, L. Y. *J. Organomet. Chem.* **2004**, *689*, 1746. (b) Neo, S. P.; Hor, T. S. A. *J. Organomet. Chem.* **1994**, *464*, 113. (c) Teo, P.; Koh, L. L.; Hor, T. S. A. *Chem. Comm.* **2007**, 4221. (d) Hor, T. S. A.; Neo, S. P.; Tan, C. S.; Mak, T. C. W.; Leung, K. W. P.; Wang, R. J. *Inorg. Chem.* **1992**, *31*, 4510. (e) Neo, S. P.; Zhou, Z. Y.; Mak, T. C. W.; Hor, T. S. A. *Inorg. Chem.* **1995**, *34*, 520.

(6) (a) Teo, P.; Koh, L. L.; Hor, T. S. A. *Inorg. Chem.* **2003**, *42*, 7290. (b) Teo, P.; Foo, D. M. J.; Koh, L. L.; Hor, T. S. A. *Dalton Trans.* **2004**, *20*, 3389. (c) Teo, P.; Koh, L. L.; Hor, T. S. A. *Inorg. Chim. Acta* **2006**, *359*, 3435. (d) Teo, P.; Koh, L. L.; Hor, T. S. A. *Chem. Comm.* **2007**, 2225. (e) Teo, P.; Koh, L. L.; Hor, T. S. A. *Inorg. Chem.* **2008**, *48*, in press.

10.1021/ic801311j CCC: $40.75
Published on Web 09/13/2008

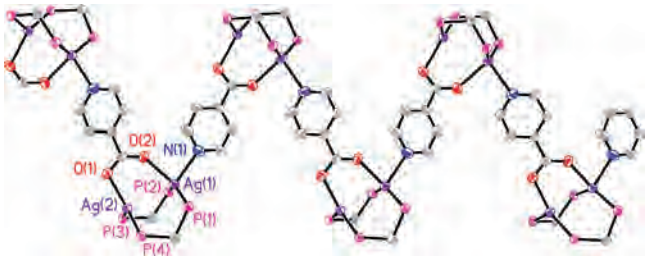

Figure 1. ORTEP drawing (50% thermal ellipsoids) of a section of the polymeric structure of $[Ag_2(isonic)(dppm)_2]_n(OTf)_n$, **1** (hydrogen atoms, anions, and phenyl rings are omitted for clarity).

Table 1. Selected Bond Lengths (Å) and Bond Angles (deg) for $[Ag_2(isonic)(dppm)_2]_n(OTf)_n$, **1**

bond lengths/Å		bond angles/deg	
Ag(1)−N(1)	2.398 (5)	N(1)−Ag(1)−P(1)	108.85(14)
Ag(1)−P(1)	2.4214 (14)	N(1)−Ag(1)−P(2)	96.03(14)
Ag(1)−P(2)	2.4359 (15)	P(1)−Ag(1)−P(2)	136.68(5)
Ag(1)−O(1)	2.470 (4)	N(1)−Ag(1)−O(2)	86.21(16)
Ag(1)−Ag(2)	2.9750 (6)	P(1)−Ag(1)−O(1)	105.28(11)
Ag(2)−O(2)	2.314 (4)	P(2)−Ag(1)−O(1)	111.39(11)
Ag(2)−P(4)	2.4154 (14)	N(1)−Ag(1)−Ag(2)	152.95(13)
Ag(2)−P(3)	2.4504 (16)	P(1)−Ag(1)−Ag(2)	88.57(4)
O(1)−C(1)	1.235(6)	P(2)−Ag(1)−Ag(2)	83.88(4)
O(2)−C(1)	1.246(7)	O(1)−Ag(1)−Ag(2)	68.93(10)
		O(2)−Ag(2)−P(4)	122.70(11)
		O(2)−Ag(2)−P(3)	107.51(11)
		P(4)−Ag(2)−P(3)	128.33(5)
		O(2)−Ag(2)−Ag(1)	92.44(10)
		P(4)−Ag(2)−Ag(1)	92.44(4)
		P(3)−Ag(2)−Ag(1)	97.14(4)
		N(1)−Ag(1)−P(1)	108.85(14)

no isonic ligand coordination. These demonstrate not only the high propensity of Ag(I) for phosphine but also diphosphine selectivity in a specific structural makeup. Ag(I) isonic complexes are known,[3a,6] but surprisingly, there is no preceding example of Ag(I) phosphine complexes with any pyridyl carboxylates.

The molecular structure of **1** shows a coordination polymer of dinuclear $[Ag_2(\mu\text{-dppm})_2]$ with isonic spacers. The carboxylate serves as a bidentate endobridge supporting the Ag_2 core, whereas the pyridyl crosses over to bind to the neighboring Ag_2. This results in a 2-D zigzag polymer. The disilver core comprises tetrahedral 18-e$^-$ and trigonal-planar 16-e$^-$ Ag(I) with a short[7] but nonbonding Ag···Ag separation of 2.9750(6) Å. The asymmetric Ag_2 core is maintained in solution, as evident from the $A_2B_2X_2$-spin pattern showing two pairs of coupled doublets in its ^{31}P NMR spectrum at 213 K (δP_A, −0.18 (dd) ($J_{P-Ag(X)} = 457$); δP_B, −0.17 (dd) ppm ($J_{P-Ag(X)} = 508$); $^2J_{P-P}$, 11 Hz). Electrospray ionization mass spectrometry (ESI-MS) analysis agrees with the formation of a Ag_2(isonic)(dppm) complex (*m*/*z* 1546.6 (100%); $[Ag_4(isonic)_2(OTf)(dppm)_2-CO_2]^+$).

All attempts to prepare **1** directly from $[Ag_2(dppm)_2(OTf)_2]$ with isonicH have resulted in a binary phosphine complex. However, under limiting phosphine conditions with Ag/dppm (2:1), isonic ligand coordination occurs to give a different form of polymer **2** as the sole product. X-ray crystallographic

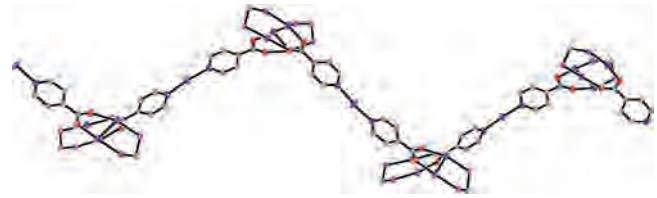

Figure 2. ORTEP drawing (50% thermal ellipsoids) of **2** (hydrogen atoms, anions, and phenyl rings are omitted for clarity).

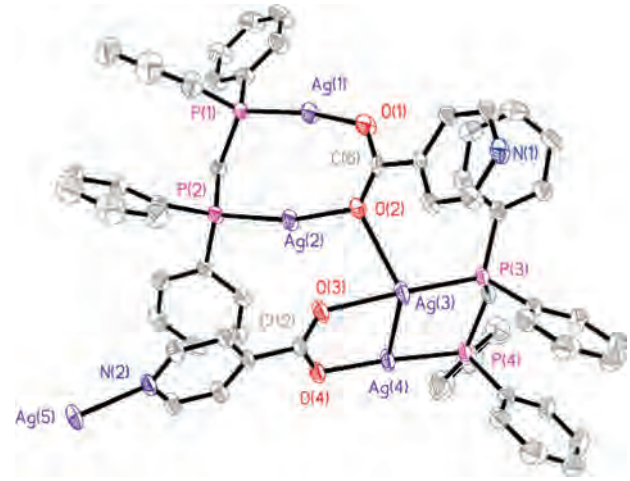

Figure 3. ORTEP drawing (50% thermal ellipsoids) of the repeating unit of Ag_5 in **2** (hydrogen atoms are omitted for clarity).

Table 2. Selected Bond Lengths (Å) and Bond Angles (deg) for $[Ag_5(isonic)_2(dppm)_2]_n(OTf)_{3n}$, **2**

bond lengths/Å		bond angles/deg	
Ag(1)−P(1)	2.3303(10)	P(1)−Ag(1)−O(1)	165.93(5)
Ag(1)−O(1)	2.119(3)	P(1)−Ag(1)−Ag(2)	89.67(3)
Ag(1)−Ag(2)	3.0266(5)	P(2)−Ag(1)−Ag(2)	91.11(3)
Ag(2)−O(2)	2.200(3)	O(1)−Ag(1)−Ag(2)	79.79(8)
Ag(2)−P(2)	2.3836(10)	O(2)−Ag(2)−P(2)	166.87(8)
Ag(3)−O(3)	2.255(3)	O(2)−Ag(2)−Ag(1)	78.84(7)
Ag(3)−P(3)	2.3798(10)	O(3)−Ag(3)−P(3)	161.23(9)
Ag(3)−O(2)	2.541(3)	O(3)−Ag(3)−O(2)	74.99(10)
Ag(3)−Ag(4)	2.9293(5)	P(3)−Ag(3)−O(2)	110.28(7)
Ag(4)−O(4)	2.120(3)	O(3)−Ag(3)−Ag(4)	74.10(8)
Ag(4)−P(4)	2.3430(10)	P(3)−Ag(3)−Ag(4)	89.66(3)
Ag(5)−N(2)	2.156(3)	O(2)−Ag(3)−Ag(4)	129.84(6)
Ag(5)−N(1)#1	2.160(3)	O(4)−Ag(4)−P(4)	175.66(9)
O(1)−C(6)	1.240(5)	O(4)−Ag(4)−Ag(3)	87.33(8)
O(2)−C(6)	1.263(5)	P(4)−Ag(4)−Ag(3)	93.79(3)
O(3)−C(12)	1.250(5)	N(2)−Ag(5)−N(1)#1	174.28(14)
O(4)−C(12)	1.253(5)		

analysis shows a highly unusual form of polymer of Ag_5 with $[Ag_5(isonic)_2(dppm)_2](OTf)_3$ as the repeating unit (Figures 2 and 3; Table 2). This is a new class of polymer-of-oligomers (POLO). It is reminiscent of the Ag_2 core except that, under limiting dppm, the isonic ligand has to fulfill the bridging role, thus giving the $[Ag_2(\mu\text{-isonic})(\mu\text{-dppm})]$ core. The phosphine deficiency also triggers the isonic ligand to raise its electron donation from oxygen in the form of a weak dative bond (2.541(3) Å; cf., Ag···$O_{carboxylate}$ avg., 2.174Å) that connects the neighboring Ag_2 moiety. The Ag_5 repeating oligomer is dissected into two Ag_2's, connected by carboxylate oxygen, and a unique pyridyl-coordinated Ag, that is $[Ag_2+Ag_2+Ag]$. The significantly shorter separation of Ag(3)···Ag(4) (2.9293(5) Å; 16e$^-$-14e$^-$) compared to Ag(1)···Ag(2) (3.0266(5); 14e$^-$-14e$^-$)

(7) (a) Burrows, A. D.; Mahon, M. F.; Palmer, M. T. *Dalton Trans.* **1998**, 1941. (b) Kall, P.; Grins, J.; Fahlman, M.; Soderlind, F. *Polyhedron* **2001**, *20*, 2747. (c) Abu-Youssef, M. A. M.; Dey, R.; Gohar, Y.; Massoud, A. A.; Ohrstrom, L.; Langer, V. *Inorg. Chem.* **2007**, *46*, 5893.

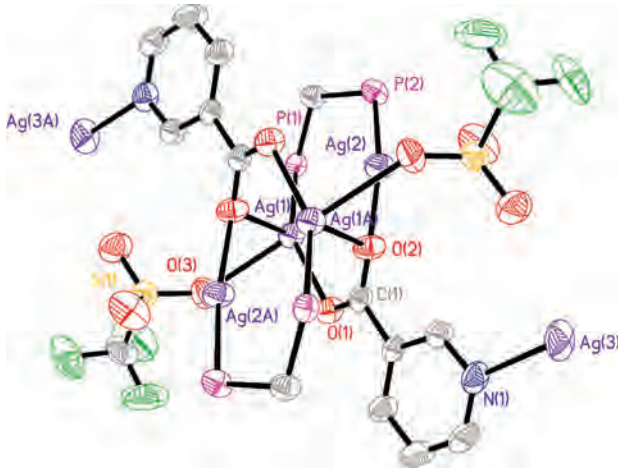

Figure 4. ORTEP drawing (50% thermal ellipsoids) of **3** (hydrogen atoms, noncoordinating anions, and phenyl rings are omitted for clarity).

Figure 5. Ball-and-stick model of **3** (hydrogen atoms and phenyl rings are omitted for clarity).

Table 3. Selected Bond Lengths (Å) and Bond Angles (deg) for $[Ag_5(Nic)_2(OTf)_2(dppm)_2]_n(OTf)_n$, **3**

bond lengths/Å		bond angles/deg	
Ag(1)−O(1)	2.266(3)	O(1)−Ag(1)−P(1)	152.48(8)
Ag(1)−P(1)	2.3853(10)	O(1)−Ag(1)−O(3)	86.25(13)
Ag(1)−O(3)	2.524(3)	P(1)−Ag(1)−O(3)	113.94(11)
Ag(1)−O(2)#1	2.592(3)	O(1)−Ag(1)−O(2)#1	87.02(10)
Ag(1)−Ag(2)	3.0360(6)	P(1)−Ag(1)−O(2)#1	115.44(7)
Ag(1)−Ag(2A)	3.173(3)	O(3)−Ag(1)−O(2)#1	74.67(12)
Ag(2)−Ag(2A)	0.731(7)	O(1)−Ag(1)−Ag(2)	82.62(7)
Ag(2)−O(2)	2.124(3)	O(3)−Ag(1)−Ag(2)	150.82(11)
Ag(2)−P(2)	2.3307(12)	O(2)#1−Ag(1)−Ag(2)	77.88(7)
Ag(2A)−O(2)	2.333(5)	O(1)−Ag(1)−Ag(2A)	79.94(9)
Ag(2A)−P(2)	2.353(4)	O(3)−Ag(1)−Ag(2A)	160.46(14)
Ag(2A)−O(5)#1	2.581(4)	O(2)#1−Ag(1)−Ag(2A)	90.77(17)
Ag(3)−N(1)#2	2.182(4)	Ag(2)−Ag(1)−Ag(2A)	13.27(12)
Ag(3)−N(1)	2.182(4)	Ag(2A)−Ag(2)−O(2)	97.4(2)
O(2)−Ag(1)#1	2.592(3)	O(2)−Ag(2)−P(2)	166.78(8)
O(5)−Ag(2A)#1	2.581(4)	Ag(2A)−Ag(2)−Ag(1)	94.1(2)
O(1)−C(1)	1.238(4)	O(2)−Ag(2)−Ag(1)	72.63(8)
O(2)−C(1)	1.271(5)	Ag(2)−Ag(2A)−O(2)	64.5(2)
		Ag(2)−Ag(2A)−O(5)#1	87.9(3)
		O(2)−Ag(2A)−O(5)#1	85.84(16)
		Ag(2)−Ag(2A)−Ag(1)	72.6(2)
		O(2)−Ag(2A)−Ag(1)	67.63(11)
		O(5)#1−Ag(2A)−Ag(1)	151.8(2)
		N(1)#2−Ag(3)−N(1)	179.998(2)

despite the higher electron deficiency of the latter could be explained by Ag−Ag bonding interactions in the former.

Isolation of **1** and **2** demonstrated that the 1,4-disposition of the two functional groups of the isonic ligand makes it a natural spacer to support unidirectional polymers. The successful replacement of dppm, which is a classical ligand in A-frame chemistry, by the carboxylate without disrupting the Ag_2 core further suggests that isonic is a suitable spacer to promote polymer chain formation with dimetal as the building block. Unlike dppm, which is strictly a $4e^-$ donor, the ability for the isonic ligand to expand its electron donation

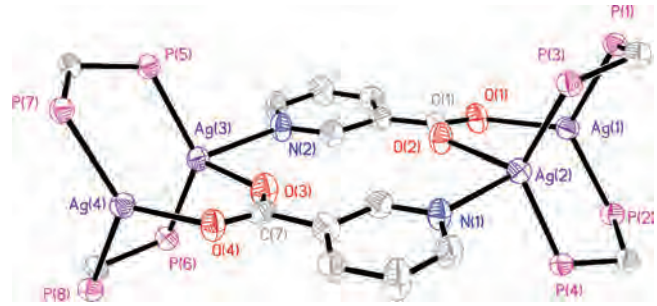

Figure 6. ORTEP drawing (50% thermal ellipsoids) of the repeating unit of $[Ag_4(Nic)_2(dppm)_4](OTf)_2$, **4** (hydrogen atoms, anions, and phenyl rings are omitted for clarity).

Table 4. Selected Bond Lengths (Å) and Bond Angles (deg) for $[Ag_4(Nic)_2(dppm)_4](OTf)_2$, **4**

bond lengths/Å		bond angles/deg	
Ag(1)−O(1)	2.301(6)	O(1)−Ag(1)−Ag(2)	88.16(14)
Ag(1)−P(1)	2.445(2)	P(1)−Ag(1)−Ag(2)	90.86(5)
Ag(1)−P(2)	2.449(2)	P(2)−Ag(1)−Ag(2)	98.47(5)
Ag(1)−Ag(2)	3.0224(8)	O(2)−Ag(2)−N(1)	87.1(2)
Ag(2)−O(2)	2.351(5)	P(3)−Ag(2)−N(1)	106.81(17)
Ag(2)−P(3)	2.435(2)	O(2)−Ag(2)−Ag(1)	71.98(13)
Ag(2)−N(1)	2.441(6)	N(1)−Ag(2)−Ag(1)	157.13(15)
Ag(2)−P(4)	2.463(2)	P(4)−Ag(2)−Ag(1)	81.41(5)
Ag(3)−O(3)	2.374(5)	O(3)−Ag(3)−N(2)	86.9(2)
Ag(3)−N(2)	2.427(6)	O(3)−Ag(3)−Ag(4)	70.46(14)
Ag(3)−P(6)	2.441(2)	N(2)−Ag(3)−Ag(4)	156.76(15)
Ag(3)−P(5)	2.451(2)	P(6)−Ag(3)−Ag(4)	88.96(5)
Ag(3)−Ag(4)	3.0048(8)	P(5)−Ag(3)−Ag(4)	83.03(5)
Ag(4)−O(4)	2.302(5)	O(4)−Ag(4)−Ag(3)	90.11(14)
Ag(4)−P(7)	2.437(2)		
Ag(4)−P(8)	2.450(2)		
O(1)−C(1)	1.259(9)		
O(2)−C(1)	1.259(9)		
O(3)−C(7)	1.253(9)		
O(4)−C(7)	1.230(9)		

through its basic oxygen allows the spacer to support electron-deficient systems such as **2**. The off-tangential coordination at the oxygen site also enables cross-linking. The network of polymer **2** is unique. The Ag_5 building block comprises a mix of linear, T-shape, and tetrahedral metal geometries supplemented by M−M interaction. This special feature would make the assembly difficult to repeat outside the d^{10} system.

The formation of **2** is a thermodynamically driven self-assembly process when the substrates are in a one-pot mixture. When dppm is increased to molar equivalence, namely, Ag/dppm (1:1), it yields $[Ag_2(OTf)(dppm)_2](OTf)$ as the only isolated product (δ_P = 9.0, 11.5 ppm; ESI-MS: *m*/*z* 1132.8, $[Ag_2(OTf)(dppm)_2]^+$), instead of the stoichiometrically favored **1**. As the latter can only be prepared with the use of Ni(II), its formation probably proceeds by phosphine transfer from Ni(II) to Ag(I) giving $[Ag_3Cl_2(dppm)_3]^+$ before isonic coordination to give the polymer chain with HCl elimination. Evidence of this comes from *in situ* observation of $[Ag_3Cl_2(dppm)_3]^+$ by ESI-MS (*m*/*z* 1546.5), NMR (δ_{31P} −1.3, −3.4 ppm), and the isolation of solid $[Ag_3Cl_2(dppm)_3]^+$ crystallized from the mixture of $NiCl_2(dppm)$ and AgOTf.[8]

(8) Franzoni, D.; Pelizzi, G.; Predieri, G.; Tarasconi, P.; Vitali, F. *Dalton Trans.* **1989**, 247.

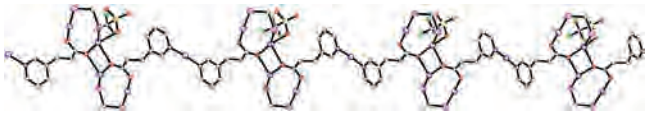

Figure 7. Ball-and-stick model of $[Ag_5(3\text{-}PyPrO_2)_2(OTf)(dppm)_2]_n(OTf)_{2n}$, **5** (hydrogen atoms, noncoordinating anions, and phenyl rings are omitted for clarity).

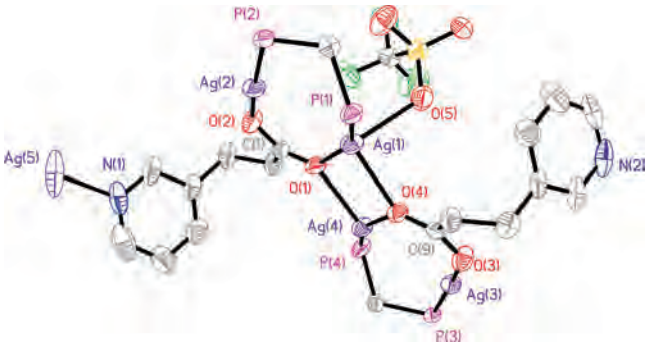

Figure 8. ORTEP drawing (50% thermal ellipsoids) of the repeating unit of $[Ag_5(3\text{-}PyPrO_2)_2(OTf)(dppm)_2]_n(OTf)_{2n}$, **5** (hydrogen atoms, noncoordinating anions, and phenyl rings are omitted for clarity).

The reaction between $[Ag_2(OTf)_2(dppm)]$ and 3-pyridylformic acid [or nicotinic acid (NicH)] gives a new form of Ag_5 polymer formulated as $[Ag_5(Nic)_2(OTf)_2(dppm)_2]_n(OTf)_n$, **3** (Figures 4 and 5, Table 3). Similar to **2**, the dinuclear $[Ag_2(\mu\text{-nic})(\mu\text{-dppm})]$ is prominent. However, instead of a side-by-side dimerization as in **1**, the two Ag_2 cores fuse together through each of its carboxylate oxygens, thus giving a metallobicyclic Ag_4 structure. This is supplemented by triflate coordination on one of the metals on Ag_2. Like **2**, the pendant pyridyl picks up a unique Ag(I), thus enabling chain propagation into a related but different form of POLO polymer of Ag_5 (or Ag_4+Ag) oligomers. Distorted sawhorse, trigonal-planar, and linear Ag(I) are evident. Saturation of a Ag center in the Ag_2 core precludes the formation of the Ag−Ag bond, thus explaining the larger Ag···Ag separation (3.173(3) Å) compared to that in **1** and **2** (Ag···Ag = 2.9750(6) for **1** and 3.0266(5) and 2.9293(5) Å for **2**). Its formation suggests that the 1,4- functional group disposition in the spacer is not a prerequisite for polymer propagation. The 1,3-orientation, despite a tighter steric demand, can also support unidirectional polymerization. This is achieved through a bicyclic Ag_2 dimerization to give a more compact Ag_4 macrocycle. The solution analysis of **3** is consistent with a pyridylcarboxylate coordinated Ag(I)−dppm complex {^{1}H NMR: δ 9.51 (s), 8.52 (d), 8.43 (d) (Py), 7.3−7.5 (m) (Ph), 1.6 (Me). ^{31}P{^{1}H} NMR: δ 14.4, 9.9, J_{P-Ag} 516, 759 Hz, $^2J_{P-P}$ 19.9, 22 Hz. ESI-MS: *m/z* (%) 721.8 (25%) ($[Ag_2(Nic)(dppm)_2]^+$, 748.8 (45%) ($[Ag_4(OTf)_2(dppm)_2]^{2+}$, 1105.7 (7%) ($[Ag_2(Nic)(dppm)_2]^+$), 1132.8 (15%) ($[(Ag_4(Nic)_2Cl_2(dppm) + H^+]^+$}. The IR analysis of **3** is within expectations ($\upsilon(COO)_{asym}$, 1631; $\upsilon(COO)_{sym}$, 1262 cm^{-1}).

Although $[Ag_2(OTf)(dppm)_2](OTf)$ gives no positive product with isonicH, it reacts readily with NicH to give a novel tetranuclear ring complex, $[Ag_4(Nic)_2(dppm)_4](OTf)_2$, **4**. It is formed by the fusion of two $[Ag_2(\mu\text{-nic})(\mu\text{-dppm})_2]$ rings through pyridyl. The meta orientation of the spacer facilitates the closed-ring structure, resulting in tetrahedral and trigonal-planar Ag(I) (Figure 6, Table 4). Similarly, no active Ag−Ag bond (Ag···Ag 3.0136 Å (avg.)) is expected in view of the electron saturation.

Table 5. Selected Bond Lengths (Å) and Bond Angles (deg) for $[Ag_5(3\text{-}PyPrO_2)_2(OTf)(dppm)_2]_n(OTf)_{2n}$, **5**

bond lengths/Å		bond angles/deg	
Ag(1)−O(1)	2.277(4)	O(1)−Ag(1)−O(4)	73.47(14)
Ag(1)−P(1)	2.4005(17)	O(1)−Ag(1)−O(5)	100.6(2)
Ag(1)−O(4)	2.479(4)	O(4)−Ag(1)−O(5)	83.35(17)
Ag(1)−O(5)	2.516(5)	O(1)−Ag(1)−Ag(2)	74.01(11)
Ag(1)−Ag(2)	3.0967(7)	P(1)−Ag(1)−Ag(2)	81.84(4)
Ag(2)−O(2)	2.094(4)	O(4)−Ag(1)−Ag(2)	145.71(10)
Ag(2)−P(2)	2.3277(17)	O(5)−Ag(1)−Ag(2)	113.21(12)
Ag(3)−O(3)	2.105(4)	O(2)−Ag(2)−Ag(1)	83.39(12)
Ag(3)−P(3)	2.3228(16)	P(2)−Ag(2)−Ag(1)	95.14(4)
Ag(3)−Ag(4)	3.0955(7)	O(3)−Ag(3)−Ag(4)	82.15(12)
Ag(4)−O(4)	2.240(4)	P(3)−Ag(3)−Ag(4)	95.71(4)
Ag(4)−P(4)	2.3980(17)	O(4)−Ag(4)−O(1)	74.64(14)
Ag(4)−O(1)	2.452(4)	O(4)−Ag(4)−Ag(3)	75.37(11)
Ag(5)−N(2)#1	2.123(6)	P(4)−Ag(4)−Ag(3)	81.61(4)
Ag(5)−N(1)	2.137(7)	O(1)−Ag(4)−Ag(3)	149.22(10)
O(1)−C(1)	1.256(7)	N(2)#1−Ag(5)−N(1)	173.3(3)
O(2)−C(1)	1.262(7)		
O(3)−C(9)	1.257(7)		
O(4)−C(9)	1.268(7)		

The chemical inequivalence of the two phosphine groups across a Ag_2 frame in **4** is evident in its room temperature ^{31}P-{^{1}H} NMR spectrum, which reveals two broad doublets [δ_P 10.9 ppm (J_{P-Ag} = 541 Hz), 6.6 ppm (J_{P-Ag} = 456 Hz)]. At 213 K, these broad peaks resolve into a complex spectrum of two major doublets of doublets and many other hitherto unidentified minor doublets.

The consistent Ag_5 polymer formation based on the Ag_2 core prompted us to test the limit of such assembly by introducing a longer spacer with greater skeletal flexibility,[6b,c] namely, 3-$PyPrO_2H$ (3-pyridylpropionic acid). This resulted in the third form of Ag_5 POLO polymer $[Ag_5(3\text{-}PyPrO_2)_2(OTf)(dppm)_2]_n(OTf)_{2n}$, **5** (Figures 7 and 8, Table 5), which is also based on the fusion of two $[Ag_2(\mu\text{-}PyPrO_2)(\mu\text{-dppm})]$ rings supplemented by an exocyclic pyridyl coordination at linear Ag(I) without formal Ag−Ag bonds (Ag···Ag = 3.0967(7) and 3.0955(7) Å). Additional triflate coordination on one of the metals in Ag_4 is evident. The longer spacer gives a Ag_4 core that is less compact compared to that of **3**. Unlike **3**, which has a center of symmetry, **5** is asymmetric, as a result of selective triflate coordination.

Polymer **5** can be considered a structural intermediate of **2** and **3**. In **2**, the two Ag_2 cores are connected side-by-side by a single oxygen. In **3**, the two Ag_2's are fused head-to-head via one oxygen across each Ag_2. In **5**, it resembles the latter by using both oxygens to promote a closer contact through a Ag_2O_2 ring formation, but it is also akin to the former by keeping the two Ag_2's apart through an edge-on dimerization.

In all of the above assemblies, the carboxylate group functions as a dppm-like bridge ligand to support the key Ag_2 core with a short Ag···Ag contact to enable it to be the fundamental building block. To test the coordinative flexibility of the carboxylate, we have replaced dppm by a diphosphine that commonly spans over longer M···M distances, namely, ferrocene-based dppf (1,1′-bis(diphe-

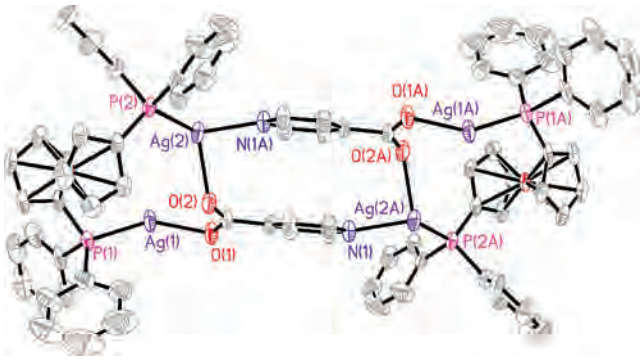

Figure 9. ORTEP drawing (50% thermal ellipsoids) of $[Ag_4(isonic)_2(dppf)_2](OTf)_2$, **6** (hydrogen atoms and anions are omitted for clarity).

Table 6. Selected Bond Lengths (Å) for $[Ag_4(isonic)_2(dppf)_2](OTf)_2$, **6**, and $[Ag_5(Nic)_2(dppf)_2](OTf)_3$, **7**

bond lengths/Å	**6**	**7**
Ag(1)−O(1)	2.258(4)	2.153(6)
Ag(1)−P(1)	2.3360(14)	2.340(3)
Ag(1)−O(3)	2.467(5)	
Ag(2)−N(1)#1	2.302(4)	
Ag(2)−P(2)	2.3498(14)	2.341(3)
Ag(2)−O(4)	2.397(5)	
Ag(2)−O(2)	2.465(4)	2.142(6)
Ag(1)−Ag(2)		3.3010(15)
Ag(3)−O(3)		2.133(6)
Ag(3)−P(3)		2.338(3)
Ag(3)−Ag(4)		3.3049(15)
Ag(4)−O(4)		2.171(6)
Ag(4)−P(4)		2.355(3)
Ag(5)−N(2)		2.140(7)
Ag(5)−N(1)		2.141(7)
O(1)−C(6)	1.245(7)	1.263(10)
O(2)−C(6)	1.245(7)	1.256(10)
O(3)−C(12)		1.268(10)
O(4)−C(12)		1.242(10)

nylphosphino)ferrocene).[9] Reaction between $[Ag_2(dppf)](OTf)_2$ and isonicH gives $[Ag_4(isonic)_2(dppf)_2](OTf)_2$, **6** (Figure 9, Tables 6 and 7), whose structure shows that the dinuclear $[Ag_2(\mu\text{-isonic})(\mu\text{-dppf})]$ core is still formed, and that two of these are dimerized to give a Ag_4 rectangle-like ring with a cavity size of 3.3 × 6.5 Å^2. The cobridging of dppf and isonic on Ag_2 is unexpected because of their contrasting ligand bite properties. This is overcome by moving one of the Ag's out of the Ag_2O_2 plane with minimum distortion on the carboxylate bridge, which also drags the phosphine out of the plane. This results in a long Ag···Ag separation (3.809 Å), which is supportable by a flexible ligand like dppf. The ability for the carboxylate to cross over such a long bridge is unexpected. Its solid-state packing shows rectangular channels created by the stacking of the cations (Figure 10).

It is notable that the reaction that yields **6** cannot proceed if dppf is replaced by dppm. This is unusual since the Ag(I) reactivity with dppm or dppf is generally similar. The unexpected differences here can only be explained by the different framework demands of the resultant products. The sharp bite angle and the short skeletal frame of dppm would not allow it to support a Ag_4 ring such as **6**. A similar phenomenon is observed in the reaction between $[Ag_2(dppf)](OTf)_2$ and NicH, giving a pentanuclear $[Ag_5(Nic)_2(dppf)_2](OTf)_3$, **7** (Ag···Ag = 3.3030 Å (avg); Figure 11, Tables 6 and 7) with two $[Ag_2(\mu\text{-nic})(\mu\text{-dppf})]$'s bridged by a linear Ag through pyridyl coordination. However, with no other active site for propagation, the product is a discrete Ag_5 with no polymerization propensity. This complex can then be viewed as the building block of the polymers observed above, especially **2**.

Table 7. Selected Bond Angles (deg) for $[Ag_4(isonic)_2(dppf)_2](OTf)_2$, **6**, and $[Ag_5(Nic)_2(dppf)_2](OTf)_3$, **7**

bond angles/deg	**6**	**7**
O(1)−Ag(1)−P(1)	151.39(13)	154.98(18)
O(1)−Ag(1)−O(3)	94.56(17)	
P(1)−Ag(1)−O(3)	111.92(12)	
O(1)−Ag(1)−Ag(2)		67.52(17)
P(1)−Ag(1)−Ag(2)		121.53(7)
N(1)#1−Ag(2)−P(2)	125.96(12)	
N(1)#1−Ag(2)−O(4)	87.59(17)	
P(2)−Ag(2)−O(4)	130.21(16)	
N(1)#1−Ag(2)−O(2)	90.08(16)	
P(2)−Ag(2)−O(2)	116.62(10)	164.19(19)
O(4)−Ag(2)−O(2)	96.2(2)	
O(2)−Ag(2)−Ag(1)		78.81(17)
P(2)−Ag(2)−Ag(1)		113.35(7)
O(3)−Ag(3)−P(3)		163.53(18)
O(3)−Ag(3)−Ag(4)		80.46(16)
P(3)−Ag(3)−Ag(4)		113.80(7)
O(4)−Ag(4)−P(4)		158.12(18)
O(4)−Ag(4)−Ag(3)		66.66(17)
P(4)−Ag(4)−Ag(3)		120.87(7)
N(2)−Ag(5)−N(1)		164.6(3)

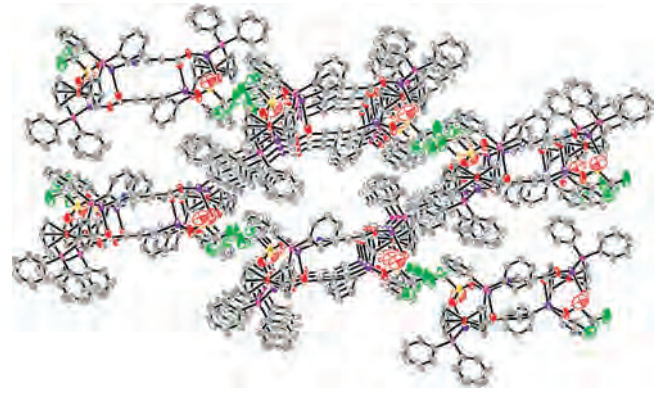

Figure 10. ORTEP packing diagram (50% thermal ellipsoids) of $[Ag_4(isonic)_2(dppf)_2](OTf)_2$, **6**, showing columns with rectangular channels (hydrogen atoms and anions not shown for clarity).

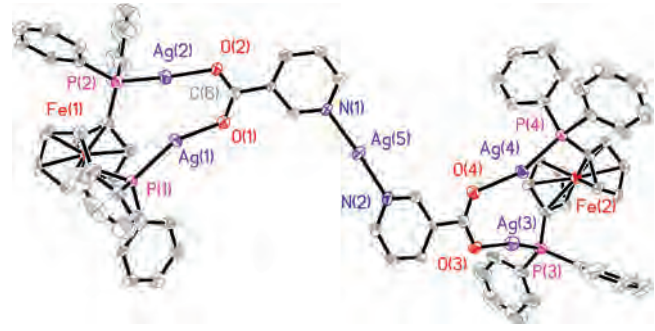

Figure 11. ORTEP drawing (50% thermal ellipsoids) of $[Ag_5(Nic)_2(dppf)_2](OTf)_3$, **7** (hydrogen atoms and anions are omitted for clarity).

(9) Chien, S. W.; Hor, T. S. A. In *Ferrocenes (Ligands, Materials and Biomolecules)*; Štěpnička, P., Ed.; Wiley: England, 2008; pp 33−116.

(10) (a) Tian, L.; Elim, H. I.; Ji, W.; Vittal, J. J. *Chem. Commun.* **2006**, 4276. (b) Zhang, Y.; Peng, H.; Huang, W.; Zhou, Y.; Yan, D. *J. Phys. Chem. C* **2008**, *112*, 2330. (c) Li, Y.; Wu, Y.; Ong, B. S. *J. Am. Chem. Soc.* **2005**, *127*, 3266. (d) Ng, M. T.; Boothroyd, C. B.; Vittal, J. J. *J. Am. Chem. Soc.* **2006**, *128*, 7118.

The solution analysis of **7** supports the formation of a nicotinate-coordinated Ag_2(dppf) complex {^{1}H NMR: δ 9.3 (s), 8.8, 8.5 (d) (Py), 7.4−7.6 (m) (Ph), 4.0, 4.5 (s) (Cp). ^{31}P{^{1}H} NMR: δ 6.4 (br). ESI-MS: *m*/*z* (%) 661.1 (100) ([Agdppf]$^+$), 891.7 (35) ([Ag_2(Nic)(dppf)]$^+$)}. The IR analysis of **7** ($\upsilon(COO)_{asym}$, 1608, $\upsilon(COO)_{sym}$, 1280, 1253) is within expectations. Similar to **6**, lowering of the temperature to 183 K resulted in the resolution of the broad resonance in the ^{31}P NMR spectrum ($\nu_{1/2}$ 300 Hz) into two broad doublets (δ 10.1, 6.1, J_{P-P} = 45 Hz).

Witnessed herein is the formation of a common Ag_2 dinuclear frame supported by the diphosphine and pyridyl carboxylates. This core can be supported by different conformational and geometric demands of the ligands. To achieve higher stabilization, the Ag_2 core undergoes dimerization to give the closed or open Ag_4, which could also add an external Ag atom to give the Ag_5 moiety. The latter, which comprises two Ag_2 and an Ag, propagates in a manner dictated by the spacer character. The presence of linear Ag(I) along the polymer chain ensures that the inter-Ag_4 contacts are minimal. This results in a remarkably consistent Ag_5 POLO polymer network across different pyridyl carboxylate and diphosphine ligands.

Oligomeric and polymeric silver complexes are generally easy to form but difficult to characterize. Some of these materials readily decompose to nanosilver, the process of which has been developed into a range of silver-based technologies.[10] Highlighted herein is a cooperative harness of the spatial features of different pyridylcarboxylate isomers and two contrasting diphosphines. Their combinative use has led to polynuclear or polymeric entities that are crystallographically characterizable. This is evident as all complexes (**1**−**7**) are structurally distinctive even though they have closely related ligands, stoichiometry, and formation conditions. Their diversity outlines the challenge ahead. It also marks an important step in the advancement of silver assemblies. Our current understanding of the molecule-to-materials process lacks structural insight at the molecular level. A major challenge in nanosilver technologies is to use structurally defined molecular materials to direct a structurally sensitive conversion process. The achievement of such would be a major milestone in the current research of silver chemistry.

Experimental Section

General Procedures. All reactions were performed under pure dry nitrogen using standard Schlenk techniques. The products are air-stable, and hence, recrystallizations were performed in the air. All chemicals used in the synthesis were of reagent-grade quality obtained from commercial sources and used as received. Commercial reagents MeOH, CH_2Cl_2, and tetrahydrofuran (THF) were predried using a commercial solvent drier. $NiCl_2$(dppm) was prepared according to literature procedures.[11]

All ^{1}H NMR (δ(TMS) 0.0 ppm) and ^{31}P{^{1}H} NMR (δ(85% H_3PO_4) 0.0 ppm) spectra were recorded at *ca.* 300 K at operating frequencies of 500.13 and 202.45 MHz, respectively, on a Bruker Avance 500 MHz apparatus. Elemental analyses were performed by the Elemental Analysis Laboratory of our department. ESI-MS spectra were obtained with a Finnigan/MAT LCQ mass spectrometer coupled with a TSP4000 HPLC system and the crystal 310 CE systems. Samples were injected via a Rheodyne valve fitted with a 5 μL sample loop. The capillary temperature was uniformly set at 70 °C for obtaining of the spectra, except that for complexes **6** and **7**, which were measured at 100 °C. Peak identifications were based on the *m*/*z* values and the isotopic distribution patterns. The *m*/*z* values given are for the most intense peak in the envelopment in each case. Samples used for elemental analyses were generally obtained directly from purified samples but may not be the single crystals used for single-crystal X-ray diffraction studies.

Syntheses. [Ag_2(isonic)(dppm)$_2$]$_n$(OTf)$_n$, 1. AgOTf (0.0385 g, 0.15 mmol) was dissolved in MeCN (3 mL) followed by the addition of CH_2Cl_2 (20 mL). $NiCl_2$(dppm) was added, and the mixture was stirred for 1 h and filtered. IsonicH was added to the filtrate and the mixture stirred overnight. The mixture was filtered, and the colorless filtrate was concentrated, followed by the addition of Et_2O. The white precipitate formed was collected by filtration (21% yield, 0.02 g). ^{31}P{^{1}H} NMR (213 K): δ −0.17 (dd) ($^1J_{P\text{-}107Ag}$ 457 Hz), −0.18 (dd) ($^2J_{P-P}$ 10.8 Hz; $J_{P\text{-}107Ag}$ 508 Hz), −3.3 (dd) ($J_{P\text{-}109Ag}$ 434). ^{1}H NMR: δ 8.9, 8.7 (s) (pyridyl); 7.31−7.94 (m) (phenyl); 4.02, 3.98, 3.61, 3.58 (Cp). ESI-MS: *m*/*z* (%) 1546.6 (100) ([Ag_4(dppm)$_2$(isonic)$_2$(OTf) − CO_2]$^+$). Anal. calcd for 1.6CH_2Cl_2: C, 42.86; H, 3.43; N, 0.79. Found: C, 43.21; H, 1.80; N, 0.28.

A pure sample of **1** could not be obtained as it is invariably contaminated by a side product of Ni(isonic)$_2$. IR measurements were not carried out as a result.

For complexes **2**, **3**, and **5**, AgOTf (0.0514 g, 0.2 mmol) was dissolved in MeOH (10 mL), followed by the addition of a THF solution (10 mL) of dppm (0.0385 g, 0.1 mmol). The mixture was stirred for 3 h to give [Ag_2(dppm)](OTf)$_2$ and the colorless solution used directly for the syntheses.

[Ag_5(isonic)$_2$(dppm)$_2$]$_n$(OTf)$_{3n}$, 2. To an aliquot of [Ag_2(dppm)](OTf)$_2$ was added isonicH (0.0123 g, 0.1 mmol), and the mixture was stirred for 3 h to give a colorless solution. The solution was evaporated to dryness, and CH_2Cl_2 was added to dissolve the white solid obtained. The mixture was filtered, and the filtrate was concentrated. Et_2O was added to precipitate out a white solid, which was collected by filtration and washed with Et_2O and dried under a vacuum (70% yield, 0.0557 g). ^{31}P{^{1}H} NMR: δ 15.1, 11.6 (br) (300 K); 13.8, 9.4, $^2J_{P-P}$ 47, 45 Hz (203 K). ^{1}H NMR: δ 8.64, 7.85 (Py), 7.3−7.5 (Ph), 2.0 (Me) (300 K). ESI-MS: *m*/*z* (%) 721.8 (20) ([Ag_2(isonic)]$^+$), 1105.6 (15) ([Ag_2(isonic)(dppm)$_2$]$^+$). IR (KBr): $\upsilon(COO)_{asym}$, 1607; $\upsilon(COO)_{sym}$, 1260 cm^{-1}. Anal. calcd for **2**·Et_2O: C, 39.97; H, 3.01; N, 1.35. Found: C, 40.19; H, 3.00; N, 1.20.

[Ag_5(Nic)$_2$(OTf)$_2$(dppm)$_2$]$_n$(OTf)$_n$, 3. To an aliquot of [Ag_2(dppm)](OTf)$_2$ was added NicH (0.0123 g, 0.1 mmol), and the mixture was stirred for 3 h to give a colorless solution. The solution was evaporated to dryness, and CH_2Cl_2 was added to dissolve the white residual solid. The mixture was filtered, and the filtrate was concentrated. Et_2O was added to precipitate out a white solid, which was collected by filtration and washed with Et_2O and dried under a vacuum (75% yield, 0.0598 g). ^{31}P{^{1}H} NMR: δ 15.0, 11.7 (br) (300 K); 14.4, 9.9, $^2J_{P-P}$ 19.9, 22 Hz (185 K). ^{1}H NMR: δ 9.51 (s), 8.52 (d), 8.43 (d) (Py), 7.3−7.5 (m) (Ph), 1.6 (Me) (300 K). ESI-MS: *m*/*z* (%) 721.8 (25) ([Ag_2(Nic)(dppm)$_2$]$^+$), 748.8 (45) ([Ag_4(OTf)$_2$(dppm)$_2$]$^{2+}$), 1105.7 (7) ([Ag_2(Nic)-

(11) Bomfim, J. A. S.; de Souza, F. P.; Filgueiras, C. A. L.; de Sousa, A. G.; Gambardella, M. T. P. *Polyhedron* **2003**, *22*, 1567.

$(dppm)_2]^+$), 1132.8 (15) ($[(Ag_4(Nic)_2Cl_2(dppm)) + H^+]^+$). IR (KBr): $\upsilon(COO)_{asym}$, 1631; $\upsilon(COO)_{sym}$, 1262 cm^{-1}. Anal. calcd for **3**·2Et_2O: C, 40.82; H, 3.38; N, 1.30. Found: C, 40.72; H, 2.98; N, 1.17.

$[Ag_4(Nic)_2(dppm)_4](OTf)_2$, 4. AgOTf (0.0514 g, 0.2 mmol) was dissolved with MeOH (10 mL), followed by the addition of a THF solution (10 mL) of dppm (0.0770 g, 0.2 mmol). The mixture was stirred for 3 h, followed by the addition of NicH (0.0123 g, 0.1 mmol), and was further stirred for 3 h and then evaporated to dryness. CH_2Cl_2 was added to dissolve the compound, and the mixture was filtered. The colorless filtrate was concentrated to *ca.* 3 mL, and Et_2O was added to precipitate out a white solid, which was collected by filtration, washed with Et_2O, and dried under a vacuum (28% yield, 0.0346 g). $^{31}P\{^1H\}$ NMR: δ 8.0 (dd) (J_{P-Ag} 602 Hz), 3.5 (dd) (J_{P-Ag} 466 Hz, $^2J_{P-P}$ 32 Hz) (213 K). ^1H NMR: δ 8.35 (b) (Py), 7.0−7.5 (m, b) (Ph) (300 K). ESI-MS: *m*/*z* (%) 1105.8 (100) ($[Ag_4(Nic)_2(dppm)_4]^{2+}$), 492.3 (47) ($[Ag(dppm)]^+$). IR (KBr): $\upsilon(COO)_{asym}$, 1600; $\upsilon(COO)_{sym}$, 1277, 1261 cm^{-1}. Anal. calcd for **4**·CH_2Cl_2: C, 53.20; H, 3.80; N, 1.08. Found: C, 52.85; H, 3.80; N, 1.08.

$[Ag_5(3\text{-}PyPrO_2)_2(OTf)(dppm)_2]_n(OTf)_{2n}$, 5. To an aliquot of $[Ag_2(dppm)](OTf)_2$ was added $PyPrO_2H$ (0.0151 g, 0.1 mmol), and the mixture was stirred for 3 h to give a colorless solution. The solution was evaporated to dryness, and CH_2Cl_2 was added to dissolve the white solid obtained. The mixture was filtered, and the filtrate was concentrated. Et_2O was added to precipitate out a white solid, which was collected by filtration and washed with Et_2O and dried under a vacuum (72% yield, 0.0592 g). $^{31}P\{^1H\}$ NMR: δ 14.9, 11.5 (br) (185−300 K). ^1H NMR: δ 8.45 (s) (Py), 7.2−7.5 (m) (Ph), 2.87, 2.55 (Me) ($^2J_{H-H}$ 6.9 Hz) (300 K). ESI-MS: *m*/*z* (%) 750.0 (95) ($[Ag_2(3\text{-}PyPrO_2)(dppm)]^+$, 1132.8 (100) ($[Ag_2(3\text{-}PyPrO_2)(dppm)_2]^+$). IR (KBr): $\upsilon(COO)_{asym}$), 1567 (br); $\upsilon(COO)_{sym}$, 1260 (br) cm^{-1}. Anal. calcd for **3**·Et_2O: C, 41.17; H, 3.31; N, 1.32. Found: C, 41.17; H, 3.15; N, 1.37.

For complexes **6** and **7**, AgOTf (0.0514 g, 0.2 mmol) was dissolved in MeOH (10 mL), followed by the addition a THF solution (10 mL) of dppf (0.0554 g, 0.1 mmol). The mixture was stirred for 5 h to give $[Ag_2(dppf)](OTf)_2$ and the orange solution used directly for the syntheses of **6** and **7**.

$[Ag_4(isonic)_2(dppf)_2](OTf)_2$, 6. To an aliquot of $[Ag_2(dppf)](OTf)_2$ was added isonicH (0.0123 g, 0.1 mmol), and the mixture was stirred for 5 h to give a yellow solution. The solution was evaporated to dryness, and CH_2Cl_2 was added to dissolve the yellow solid obtained. The mixture was filtered, and the filtrate was concentrated. Et_2O was added to precipitate out a yellow solid, which was collected by filtration and washed with Et_2O and dried under a vacuum (35% yield, 0.0364 g). $^{31}P\{^1H\}$ NMR: δ 5.3 (br) (300 K); 7.3, 3.3, $^3J_{P-P}$ 62 Hz (193K). ^1H NMR: δ 8.83, 8.11 (d) (Py), 7.4−7.6 (m) (Ph), 4.50, 3.92 (s) (Cp) (300 K). ESI-MS: *m*/*z* (%) 1232.8 (100) ($[Ag_4(isonic)_2(dppf) - H^+]^+$). IR (KBr): $\upsilon(COO)_{asym}$, 1599; $\upsilon(COO)_{sym}$, 1280, 1258 cm^{-1}. Anal. calcd for **6**: C, 47.29; H, 3.10; N, 1.35. Found: C, 46.88; H, 3.13; N, 1.50.

$[Ag_5(Nic)_2(dppf)_2](OTf)_3$, 7. To an aliquot of $[Ag_2(dppf)](OTf)_2$ was added NicH (0.0123 g, 0.1 mmol), and the mixture was stirred for 5 h to give a yellow solution. The solution was evaporated to dryness, and CH_2Cl_2 was added to dissolve the yellow solid obtained. The mixture was filtered, and the filtrate was concentrated. Et_2O was added to precipitate out a yellow solid, which was collected by filtration and washed with Et_2O and dried under a vacuum (67% yield, 0.0623 g). $^{31}P\{^1H\}$ NMR: δ 6.4 (br) (300 K); 10.1, 6.1, $^3J_{P-P}$ 45 Hz (183 K). ^1H NMR: δ 9.3 (s), 8.8, 8.5 (d) (Py), 7.4−7.6 (m) (Ph), 4.0, 4.5 (s) (Cp) (300 K). ESI-MS: *m*/*z* (%) 661.1 (100) ($[Ag(dppf)]^+$), 891.7 (35) ($[Ag_2(Nic)(dppf)]^+$)). IR (KBr): $\upsilon(COO)_{asym}$, 1608; $\upsilon(COO)_{sym}$, 1280, 1253 cm^{-1}. Anal.

Table 8. Relevant Crystallographic Data for Complexes **1**−**7**

	1	**2**	**3**	**4**	**5**	**6**	**7**
empirical formula	$C_{61.75}H_{59}Ag_2Cl_{0.50}F_3NO_2P_4S$	$C_{66}H_{54}Ag_5Cl_2F_9N_2O_{14}P_4S_3$	$C_{33.5}H_{28}Ag_{2.5}Cl_2F_{4.5}NO_{6.5}P_2S_{1.5}$	$C_{120}H_{108}Ag_4Cl_{12}F_6N_2O_{10}P_8S_2$	$C_{72}H_{66}Ag_5Cl_9F_9N_2O_{14}P_4S_3$	$C_{42}H_{33}Ag_2Cl_3F_3FeNO_5P_2S$	$C_{84}H_{68}Ag_5Cl_4F_9Fe_2N_2O_{13}P_4S_3$
temp (K)	223(2)	293 (2)	223 (2)	223 (2)	223 (2)	223 (2)	223 (2)
fw	1341.50	2100.42	1084.67	3020.84	2310.38	1160.63	2509.32
cryst syst	monoclinic	orthorhombic	triclinic	monoclinic	orthorhombic	triclinic	triclinic
space group	$P2(1)/n$	$Pbca$	$P\bar{1}$	C/c	$P2(1)2(1)2(1)$	$P\bar{1}$	$P\bar{1}$
unit cell dimensions:	15.3562 (18)	16.9859 (6)	12.0277 (7)	19.8171 (7)	16.4613 (11)	11.1836 (4)	13.911 (8)
a (Å)							
b (Å)	2.0117 (14)	28.2770 (10)	13.4108 (7)	28.4445 (10)	16.8940 (11)	12.7135 (5)	14.966 (8)
c (Å)	33.175 (4)	31.3099 (11)	15.1329 (8)	24.3506 (9)	30.899 (2)	17.4393 (6)	22.841 (13)
α (deg)	90	90	100.643 (1)	90	90	71.7130 (10)	92.605 (13)
β (deg)	97.114 (3)	90	113.164 (1)	111.737 (1)	90	79.4530 (10)	104.433 (15)
γ (deg)	90	90	102.926 (1)	90	90	72.4690 (10)	91.297 (14)
V (Å^3)	6072.1 (12)	15038.5 (9)	2083.6 (2)	12750.1 (8)	8593 (1)	2283.74 (14)	4597 (4)
Z	4	8	2	4	4	2	2
D_{calcd} (mg/m^3)	1.467	1.855	1.729	1.574	1.786	1.688	1.813
abs coeff (mm^{-1})	0.864	1.603	1.511	1.055	1.531	1.509	1.682
F (000)	2728	8272	1068	6080	4568	1152	2480
no. of reflections	42266	102217	27116	45206	60760	30379	49375
cryst size (mm^3)	0.52 × 0.24 × 0.20	0.40 × 0.20 × 0.10	0.50 × 0.30 × 0.24	0.10 × 0.06 × 0.04	0.40 × 0.36 × 0.06	0.38 × 0.12 × 0.10	0.50 × 0.08 × 0.03
index ranges	$-19 \le h \le +18$	$-18 \le h \le +22$	$-15 \le h \le +15$	$-25 \le h \le +14$	$-21 \le h \le +21$	$-14 \le h \le +14$	$-16 \le h \le +16$
	$-13 \le k \le +15$	$-36 \le k \le +35$	$-17 \le k \le +17$	$-36 \le k \le +36$	$-21 \le k \le +21$	$-16 \le k \le +16$	$-17 \le k \le +17$
	$-43 \le l \le +42$	$-40 \le l \le +36$	$-19 \le l \le +19$	$-31 \le l \le +31$	$-28 \le l \le +40$	$-22 \le l \le +22$	$-27 \le l \le +27$
R, wR^2 (all data)	0.1087, 0.1792	0.0682, 0.1025	0.0558, 0.1436	0.0724, 0.1412	0.0725, 0.1385	0.0914, 0.1665	0.1244, 0.1603
final R, wR^2 (for $I > 2\sigma$)	0.0670, 0.1608	0.0448, 0.0939	0.0470, 0.1373	0.0549, 0.1281	0.0532, 0.1293	0.0705, 0.1565	0.0698, 0.1392
largest diff peak and hole (e Å^{-3})	1.061 and −0.590	1.181 and −0.641	1.223 and −0.767	1.080 and −0.741	1.653 and −1.326	1.105 and −0.906	0.946 and −0.903

calcd for **7**·2Et_2O: C, 43.93; H, 3.40; N, 1.13. Found: C, 43.93; H, 3.18; N, 2.43.

Crystal Structure Determinations. The diffraction experiments were carried out on a Bruker SMART CCD diffractometer with a Mo Kα sealed tube at −50 °C. The program SMART[12] was used for collecting frames of data, indexing reflections, and determining lattice parameters; SAINT was used for integration of the intensity of reflections and scaling; SADABS[13] was used for absorption correction; and SHELXTL[14] was used for space group and structure determination and least-squares refinements on F^2. For complex **1**, the crystal is monoclinic, space group *P*2(1)/*n*. The asymmetric unit contains one dinuclear cation $[Ag_2(dppm)_2(isonic)]^+$ and one OTf anion. Residual solvent peaks were fitted with a disordered pair of hexane (0.75) and CH_2Cl_2 (0.25) and refined with restraints in bond lengths and thermal parameters. Final R values are R1 = 0.0690 and wR2 = 0.1954. The largest residual peak of 1.1 e^- is located near the disordered solvent hexane. The cation is linked by the nicotinate through the COO^- (with one O to each Ag) and the N (to Ag1 only). This results in a linear polymeric zigzag chain of the two. For **2**, the crystal is orthorhombic, space group *Pbca*. The asymmetric unit contains one unit complex cation $[Ag_5(dppm)_2(NC_5H_4COO)_2]$, three OTf anions, and one CH_2Cl_2. One of the OTf's and the CH_2Cl_2 appeared to be disordered and were fitted with rocking disorder structures. The complex cations pack to give a linear zigzag chain. Final R values are R1 = 0.0448 and wR2 = 0.103. For **3**, the crystal is triclinic, space group $P\bar{1}$. The crystal was observed to be losing solvent slowly during data collection. However, the data quality appeared to be good. Initial refinement showed a large residue near Ag(2). There was also a large number of solvent residual peaks. These problems were solved by (a) treating Ag(2) as disordered into two parts, the minor part having 0.15 occupancy, and (b) the solvent $CHCl_3$, which is near the symmetry point, is disordered into three sets with occupancies of 0.5:0.25:0.25. With this disorder scheme, final refinement went well to give R1 = 0.047 and wR2 = 0.144. The asymmetric unit contains the complex $[Ag_2(NC_5H_4COO)(OTf)(dppm)\cdot Ag_{0.5}]$, and another $(OTf)_{0.5}$, which is at a point of symmetry. One disordered $CHCl_3$ is also present, which is also near the point of symmetry. A polymer chain linked through N−Ag−N linkages is obtained by applying the "grow" function of SHELXTL, on the cation. For **4**, the crystal is monoclinic with space group *Cc*. The asymmetric unit contains one complex cation of $[Ag_4(NC_5H_4CO_2)_2(dppm)_4]^{2+}$, two OTf anions, and six CH_2Cl_2's. All of the CH_2Cl_2's have high thermal parameters and poor bond distances, probably due to poor packing. Three of the CH_2Cl_2's were assigned as disordered. Restraints in bond distances and thermal parameters were applied in the final refinement. Final R values are R1 = 0.0549 and wR2 = 0.1281 for a $2\theta_{max}$ of 55°. For **5**, the crystal is orthorhombic with space group *P*2(1)2(1)2(1). The asymmetric unit contains one complex cation containing five Ag(I)'s, three OTf anions, and three CH_2Cl_2's. Two of the CH_2Cl_2's are disordered. On packing, the cations form a linear polymeric chain through Ag(5)−N2 linkages along the *b* axis. Final R values are R1 = 0.0532 and wR2 = 0.1293 for a $2\theta_{max}$ of 55°. For **6**, the crystal is triclinic, space group $P\bar{1}$. The asymmetric unit contains one-half of the complex $[Ag_2(dppf)(NC_5H_4COO)](OTf)$. The whole complex is obtained by growing through the point of symmetry. There is also one $CHCl_3$ in the asymmetric unit. This $CHCl_3$ has large thermal parameters, indicating that it is loosely packed. The final R values are R1 = 0.0705 and wR2 = 0.166. For **7**, the crystal is triclinic, space group $P\bar{1}$. The asymmetric unit contains one complex cation $[Ag_5(dppf)_2(NC_5H_4COO)_2]$, three OTf anions, and two CH_2Cl_2's. The final R values are R1 = 0.0698 and wR2 = 0.1392. Relevant crystallographic information of the complexes is given in Table 8.

IC801311J

(12) *SMART Software Reference Manual*; *SAINT Software Reference Manual*, version 5.611; Bruker Analytical X-Ray Systems Inc.: Madison, WI, 2000.

(13) Sheldrick, G. M. *SADABS, software for empirical absorbtion correction*; University of Göttingen, Göttingen, Germany, 2000.

(14) *SHELXTL Reference Manual*, version 5.1; Bruker Analytical X-Ray Systems Inc.: Madison, WI, 1997.